Available online at www.sciencedirect.com
ScienceDirect
Ceramics International 35 (2009) 2775–2780
CERAMICS INTERNATIONAL
www.elsevier.com/locate/ceramint

Pressureless sintering and mechanical properties of SiO_2–Al_2O_3–MgO–K_2O–TiO_2–F (CaO–Na_2O) machinable glass–ceramics

B. Ashouri Rad, P. Alizadeh *

School of Engineering, Tarbiat Modares University, P.O. Box 14115-143, Tehran, Iran

Received 30 January 2009; received in revised form 19 February 2009; accepted 13 March 2009
Available online 15 April 2009

Abstract

To develop a high strength machinable glass–ceramic through pressureless sintering, the glassy compositions were obtained by mixing a mica-based frit and a frit in the SiO_2–CaO–Na_2O system. According to XRD results, the glass compositions mainly crystallized into phlogopite and diopside after sintering. The optimum sintered glass–ceramic with desirable mechanical properties, machinability and sinterability was achieved by addition of 30 wt.% SiO_2–CaO–Na_2O glass powder to 70 wt.% mica glass composition. SEM results confirmed presence of needle-like diopside crystals which played a reinforcement role to the platelet phlogopite and glassy matrix combination. The measurements showed bending strength and fracture toughness enhanced up to 144.6 ± 17.6 MPa and 1.7 ± 0.2 MPa $m^{1/2}$, respectively.

Keywords: B. Diopside; B. Phlogopite; C. Mechanical properties; D. Glass–ceramics

1. Introduction

Fluormica glass–ceramics are well-known materials and show a favorable combination of thermal, electrical and biomedical properties. These materials can be easily cut, drilled and turned with conventional tools. Laminated structure of mica crystals is, directly responsible for the desirable machinability because they cleave easily along the interfaces between layers while being machined [1–4].

Recently much interest has been focused on mica glass–ceramics but the mechanical strength of these materials is fairly poor. Accordingly, numerous attempts have been made to improve this disadvantage through modification of composition. Most of the commercial machinable glass–ceramics are based on potassium fluorphlogopite. Uno et al. [5] investigated barium–fluorphlogopite with higher mechanical strength and toughness in comparison with conventional potassium–fluorphlogopite. Likely, several investigations have been conducted to produce calcium–mica with enhanced mechanical properties [6–8]. Utilization of high strength phases was adjusted to prepare high strength mica glass–ceramics. The strengthening effect of additives such as titania and celsian powders has been studied via sintering method. Herein, the strength successfully improved by suppressing the longitudinal growth of mica crystals [9]. Recent study revealed that incorporating suitable amounts of Y-PSZ into mica base glass–ceramic, could result in simultaneous improvement in bending strength and fracture toughness [10]. Fabrication of oriented mica containing glass–ceramics using extrusion or hot press was another approach carried out for fulfillment of this purpose [11,12].

Efforts have been continuing to overcome these problems and to develop new mica glass–ceramics that will exhibit better performance. In this respect the addition of second glass frit to mica-based frit and sintering the obtained mixtures has still attracted less attention. Recently, Alizadeh et al. [13] have presented the pressureless sintering of apatite-based frit (viz. SiO_2–CaO–P_2O_5–MgO glass system) and mica-based glass mixture.

In the current study we attempted to improve the mechanical properties of machinable glass–ceramics by final precipitation of high strength crystalline phases along with the cleavable

* Corresponding author. Tel.: +98 21 82884399.
E-mail address: p-alizadeh@modares.ac.ir (P. Alizadeh).

0272-8842/$36.00
doi:10.1016/j.ceramint.2009.03.027

Table 1
Chemical composition of glasses (wt.%).

Glass	SiO_2	CaO	Al_2O_3	MgO	K_2O	Na_2O	B_2O_3	TiO_2	Fe_2O_3	WO_3	F
G1	37.96	–	15.36	18.08	7.57	–	6.32	5.68	–	–	9.03
G2	59.68	27.25	–	–	–	5.08	–	–	6.00	2.00	–

mica crystals. This objective was fulfilled through mixing of glassy powder in the system SiO_2–CaO–Na_2O which has been known for appropriate mechanical properties after crystallization [14], to mica-based glass composition [15], and followed by pressureless sintering. Subsequently, the sintering behavior of powder mixtures and the mechanical properties of obtained glass–ceramics were investigated.

2. Experimental procedures

2.1. Glass preparation

Glasses were prepared by fusing reagent grade chemicals. The chemical compositions of the two initial glasses are displayed in Table 1. As mentioned previously, the primary G1 and G2 glass compositions were chosen by considering good machinability and high mechanical strength, respectively. The weighed glass batches (200 g) were well mixed in an alumina jar-mill for 3 h, calcined at 900 °C for 1 h and thereafter melted in a platinum crucible at temperature ranging from 1400 to 1430 °C in an electric furnace for 30 min. The molten glasses were then quenched in cold distilled water to obtain glassy frits. Then the two obtained frits were ground in a high-speed alumina mill separately and sieved (<38 μm).

2.2. Preparation of glass mixtures

The G1 and G2 pulverized frits were mixed thoroughly using jar-mill for 6 h in an ethanol environment and dried at 130 °C for 24 h. Various weight percentages of the two frits in prepared composition resulted after mixing were given in Table 2. All compositions after milling and mixing had amorphous nature, confirmed by XRD. The glass powders were mixed with 2.5 wt.% PVA as a binder and cold pressed using a laboratory uniaxial hydraulic press into 3 mm × 7 mm × 30 mm bars and 10 mm in diameter pellets at a final pressure of 60 MPa.

2.3. Methods of analysis

The particle size distribution of the powders was determined using a particle size analyzer (Fritsch, Analysette 22). The green compacts were heat treated at a rate of 5 °C/min up to 450 °C and after soaking for 1 h, the heating rate was changed into 10 °C/min till their maximum sintering temperature reached. Then the compacts were soaked for 180 min at the sintering temperature.

Table 2
Composition of prepared glasses from mixing of two frits (wt.%).

Glass	GCM	GC10	GC20	GC30	GC40	GC50	GC60
G1	100	90	80	70	60	50	40
G2	0	10	20	30	40	50	60

The bulk density of sintered specimens was determined by Archimedes' method, using water as the immersion medium and average value of five samples was reported. The true density of powdered glass–ceramics was measured by pycnometery. The crystalline phases precipitated during sintering, were identified by XRD (Philips X'Pert) with Cu Kα radiation. Silicon powder was used as a standard material for semi-quantitative measurements. The polished and chemically etched surface of sintered glass–ceramics was observed by SEM (Philips XL30) attached with EDAX unit.

A Vickers micro-hardness tester with a diamond pyramid (Buehler Micromet I) was used to measure micro-hardness. The load was 500 g and the loading time was 30 s. At least 15 indentations were made to obtain an average value of each specimen. The flexural strength and fracture toughness of the glass–ceramics were performed using three-point bending and single edge-notched bars (SENB) methods, respectively. At least seven polished rectangular bars with dimension of 2.5 mm × 5 mm × 25 mm were used for each examination. A nearly 2.5 mm notch was made using a low speed diamond saw (Buehler Isomet) for SENB test specimens according to ASTM E399. The nominal thickness of created notch was 0.3 mm. The measurements were carried out in room temperature and the crosshead speed and span length were 1 mm/min and 20 mm, respectively (Instron Universal Testing Machine 1196). The machinability was evaluated initially by naked eye observation and then determined by calculating of relative intensity of mica crystallized phase to pure silicon according to XRD patterns.

3. Results and discussion

3.1. Sintering and crystallization

Sintering rate of compacted powders is reversely proportional to particle size of the glassy powders [16]. The mean particle size of the mixed powders at present work were determined about 6–8 μm. Fig. 1 depicts the particle size distribution of GC40 glass powder which has a mean particle size of 7 μm.

Sintering characteristics of all glass compositions have been tabulated in Table 3. It can be observed that gradual addition of CaO–SiO_2–Na_2O glass to mica glass composition decreases the optimum sintering temperature of all glass compositions in comparison with pure mica composition. As we know viscous flow is the predominant mechanism of sintering in glass and

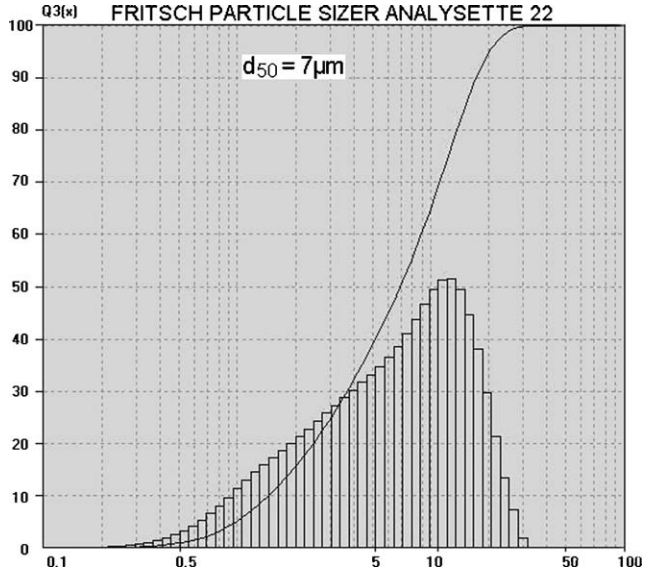

Fig. 1. Particle size distribution of the GC40 glass powder.

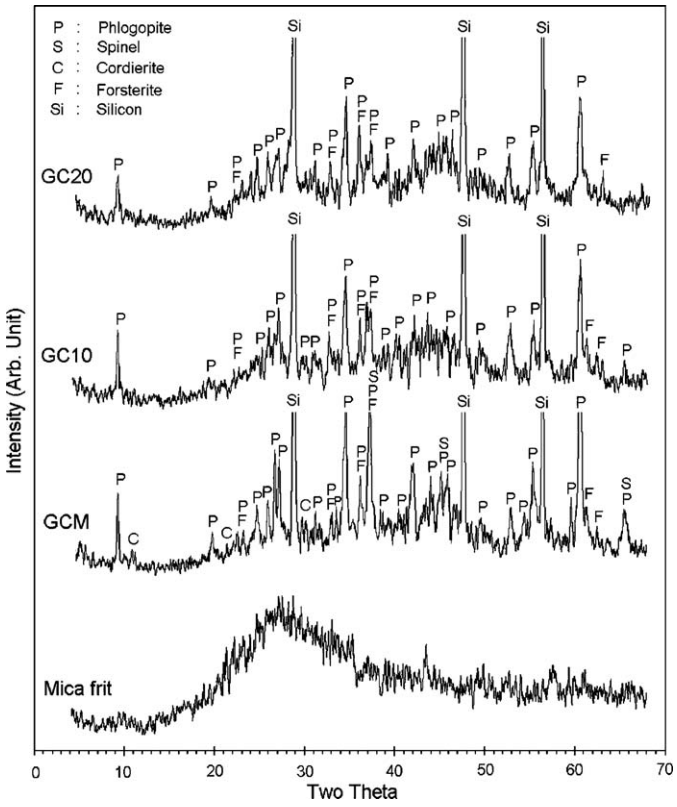

Fig. 2. XRD pattern of mica frit, GCM, GC10 and GC20 glass–ceramics.

glass–ceramic materials. It can be elucidated that incorporation of G2 glass into mica-based glass, acts as a flux and accelerates the viscous flow process, leading to lower temperature densification especially in lower amounts of G2 glass. Relative density moderately increases to maximum value in GC30 and then drops markedly in GC50 and GC60 specimens. This behavior can probably be explained by presence of higher glassy phase in the grain boundaries and formation of some crystalline phases which are precipitated by further amounts of G2 glass in two latter samples [17]. Additionally, crystallization of high-density crystalline phase from low-density residual glass during the final stage of sintering incorporates further porosity into the matrix and decreases relative density.

Figs. 2 and 3 show the XRD pattern of all prepared glass–ceramics in their optimum sintering temperature. It is clear form Fig. 2 that mica frit maintains its glassy nature during milling and mixing processes. As can be seen phlogopite is the major crystalline phase in the GCM, GC10 and GC20 specimens. Besides the phlogopite phase, very faint trace of spinel and cordierite were observed in specimen GCM. However these minor phases did not crystallize in GC10 and GC20 samples due to lower temperature of sintering. Diopside appears in the specimen GC30 and increases gradually toward GC60. Oppositely phlogopite decreases gradually as G2 glass portion increases and finally disappears entirely in GC60 specimen. In fact in sample GC60 where weight portion of G2 glass is predominant, only diopside phase is crystallized. Disappearing of mica crystals can be resulted in deterioration of some mechanical properties such as, machinability and fracture toughness. In addition, XRD pattern indicates that in all sintered glass–ceramics forsterite has been crystallized as a minor phase which mainly precipitates in magnesia–alumina–silicate systems [10,13,15].

As we know, the ions Ca^{2+} and Mg^{2+} migrate from G2 and G1 glass, respectively to form diopside crystalline phase with the chemical composition of $CaO{\cdot}MgO{\cdot}2SiO_2$ [13]. It is clear that, the constituent ion Si^{4+} can be provided from both parent glasses. Thereby it can be concluded that two glasses have been mixed completely and mutual diffusion of basic constituent existing in two glasses has been performed properly.

Formation of diopside from such well-mixed glass is dependant to crystallization of mica crystals. It was reported that [18], mica crystals are crystallized in lower temperatures than densification temperature of sintered glass–ceramic. Thus it is conceivable that initially precipitated mica crystals, act as a site for nucleating of diopside phase. As the temperature increases, diopside phase are crystallized through interaction of

Table 3
Sintering characteristics of prepared glass–ceramics.

Sintering parameters	GCM	GC10	GC20	GC30	GC40	GC50	GC60
Sintering temperature (°C)	1070	1020	1020	1020	1050	1060	1060
Linear shrinkage (%)	19.22	17.25	16.67	16.55	17.06	17.64	16.40
Bulk density (g/cm^3)	2.58	2.57	2.59	2.68	2.68	2.60	2.63
Relative density (%)	96.21	96.25	96.28	98.17	96.45	92.53	91.72

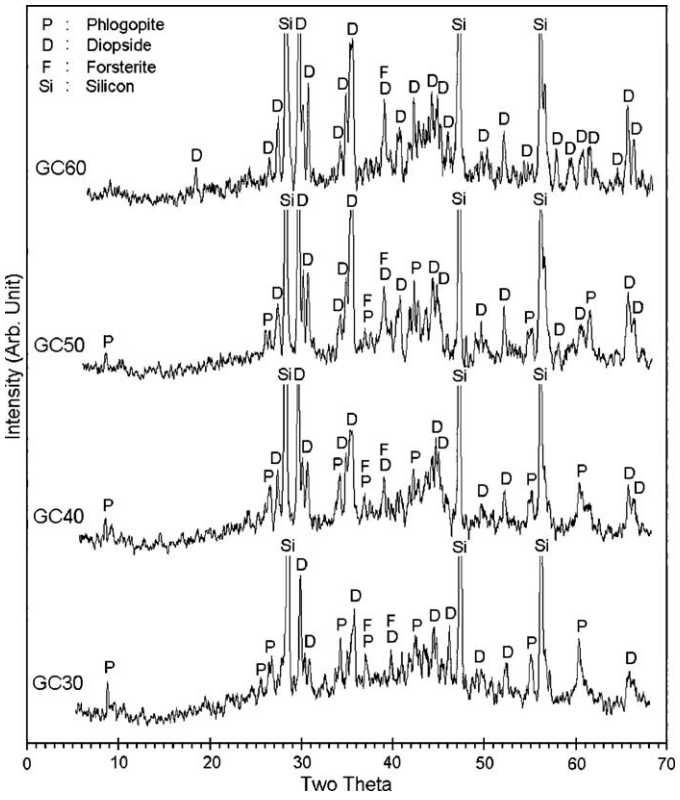

Fig. 3. XRD pattern of GC30, GC40, GC50 and GC60 glass–ceramics.

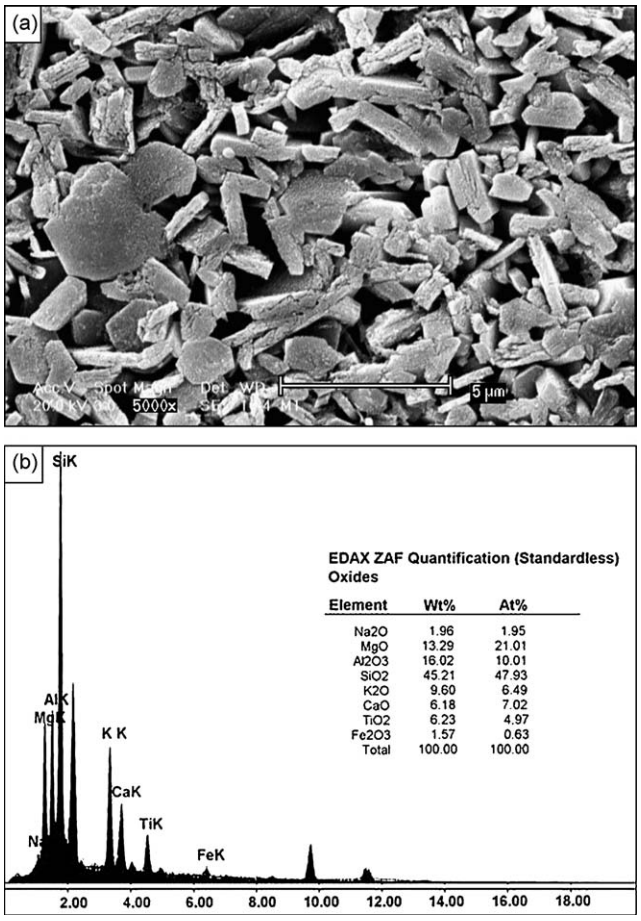

Fig. 4. SEM image (5000×) (a) and EDAX analysis of GCM specimen (b).

contemporary precipitated mica plates and glassy matrix. Consumption of mica structural constituents and growth of diopside on it lead to formation of pores in samples when higher amounts of G2 glass are used in these compositions.

In other words, specimens containing high-density crystalline phases such as diopside in great amounts are generally more susceptible to, pore formation. In this case prominent difference in density of crystallized phase and glassy matrix is responsible for pore origination and total decrease in relative density of sintered glass–ceramics.

3.2. Microstructural studies

Fig. 4a shows SEM photograph of single phase microstructure of GCM sintered specimen. The two dimensional plate-like phlogopite crystals precipitate throughout the glassy matrix and form the house of card microstructure which is, direct responsible for good machinability. Fig. 4b depicts the EDAX analysis of plate-like shaped crystalline phase in the GCM specimen. Higher amounts of Al_2O_3 and K_2O in these crystals confirmed the composition of mica phase. Fig. 5a reveals the microstructure of other single phase sintered glass–ceramic, GC60 specimen, consisted of one dimensional fibrous crystals of diopside which were locked within each other drastically. Fig. 5b demonstrates EDAX analysis of fibrous-shaped crystals in the GC60 microstructure. The fibrous phases were found to be diopside crystals due to CaO and MgO rich composition. Fig. 6 exhibits the microstructure of specimen GC40 where, the plate-like crystals of mica accompanied by the fibrous diopside crystals. In this sample, the alignment of fibrous diopside and plate-like mica crystals is very similar together and causes such uniform microstructure. The existence of other elements such as Na, Ti and Fe in composition of crystalline phases according to EDAX analysis is probably emanated from mother glass composition.

3.3. Mechanical properties

Mechanical properties as well as relative intensity of mica and diopside to pure silicon powder have been summarized in Table 4. The measured value of bending strength shows that, addition of G2 up to 30 wt.% increases bending strength sharply and then decreases it slowly. The initial improvement in bending strength could be attributed to formation of diopside crystals with interlocked needle-like structure which act as a reinforcement to mica/glass matrix. It is found that introduction of calcium-containing glass to mica glass composition could lead to formation of calcium–potassium mica solid solution after crystallization [13]. Partially substitution of K^+ ions by Ca^{2+} ions in the weak cleavage layer results in higher bonding in the silicate layers and correspondingly raises the bending strength. EDAX analysis results of mica crystals in Fig. 4b confirm partially diffusion of Ca^{2+} ions into mica crystals and formation of mica solid solution with enhanced mechanical strength. Deterioration of bending strength after GC30 brought

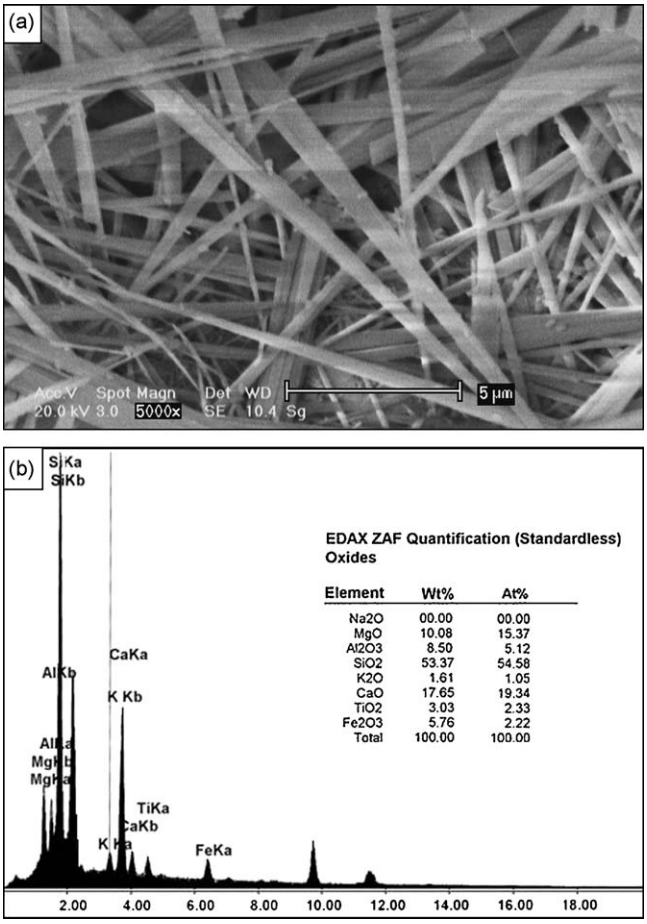

Fig. 5. SEM image (5000×) (a) and EDAX analysis of GC60 specimen (b).

about by probable formation of porosity despite higher contents of diopside phase. The microstructure of sintered glass–ceramics may also affect the strength. The interlocking of phlogopite plates coupled with a relatively high degree of needle-like diopside crystals promotes the highest mechanical strength in GC30 specimen.

The use of small number of test samples for determination of the bending strength, might result in an overlapping in measured values due to statistical nature of defects in brittle materials such glass–ceramics. As a consequence the difference in measured flexural strength might not originate from microstructural effects, but from statistical consideration. Therefore the standard deviation for sintered specimens as well as average value has been reported in Table 4.

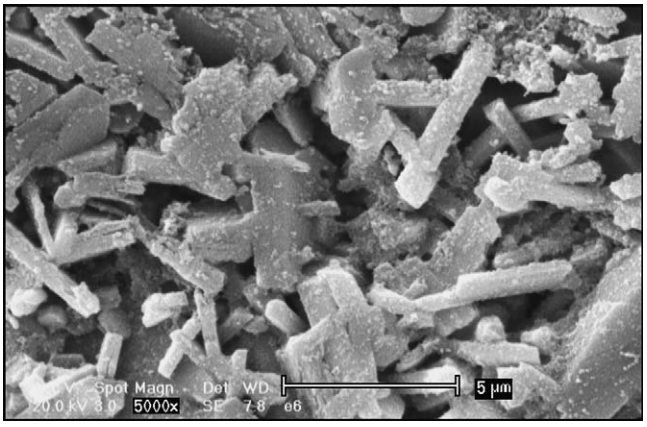

Fig. 6. SEM image (5000×) of GC40 specimen.

The fracture toughness of GCM specimen is relatively high. This behavior can be elucidated by interlocking and plate-like microstructure of phlogopite which plays a significant role in deflection and branching of cracks. By considering lower sintering temperature and relative intensity of crystallized mica to silicon in GC10 specimen which lead to lower degree of crystallinity, fracture toughness drops suddenly in contrast with CCM specimen. In the sample GC30 adequate contents and concurrent occurrence of phlogopite and diopside in microstructure deflect the cracks effectively and heighten the K_{1C} value to 1.7 ± 0.2 MPa $m^{1/2}$ which is maximum value in all obtained glass–ceramics. As it mentioned in bending strength, reduction of relative density in GC40 to GC60, also has detrimental effect on fracture toughness. Furthermore gradual reduction of phlogopite in these samples obstructs the toughening effect of interlocking plates.

It has been observed experimentally that if notch are cut too thick, the values of fracture toughness determined are systematically too high [19]. Thus the fracture toughness values measured in SENB method could be overestimated. In as much as, the same notch radius has been achieved in all specimens, a comparison between sintered glass–ceramics can be made.

Based on Table 4 results, higher amounts of precipitated diopside tend to harden the sintered bodies due to higher modulus of elasticity of diopside than phlogopite [20].

It is pointed out that, machinability of mica-based glass–ceramics is related to mica volume percentage and degree of interlocking of crystalline phase [3,21,22]. According to I_{mica}/I_{si} results and micro-hardness values in Table 4, machinability is

Table 4
Some properties of each specimen fired at their optimum sintering temperature.

Samples	Vickers micro-hardness (GPa)	Bending strength (MPa)	Fracture toughness (MPa $m^{1/2}$)	I_{mica}/I_{si}	$I_{diopside}/I_{si}$	Machinability
GCM	2.2 ± 0.9	77.5 ± 6.7	1.4 ± 0.1	0.22	0.00	Excellent
GC10	2.9 ± 0.8	97.2 ± 6.2	1.0 ± 0.1	0.19	0.00	Good
GC20	3.6 ± 0.5	107.1 ± 11.0	1.3 ± 0.1	0.15	0.00	Good
GC30	4.1 ± 0.5	144.6 ± 17.6	1.7 ± 0.2	0.13	0.32	Good
GC40	4.9 ± 0.7	131.9 ± 16.5	1.4 ± 0.2	0.10	0.39	Good
GC50	6.1 ± 0.9	126.4 ± 17.3	1.3 ± 0.1	0.07	0.50	Moderate
GC60	6.9 ± 0.9	121.6 ± 19.5	1.3 ± 0.1	0.00	0.53	Moderate

deteriorated from GCM to GC60 generally. Gradual precipitation of diopside phase from GC30 to GC60 also decreases the degree of interlocking of mica crystals and consequently impairs the machinability. These results are compatible with the result obtained by naked eye observation. Moderate machinability in GC50 and GC60 in spite of greater micro-hardness and less cleavable mica crystals is attributed to higher amounts of porosity which randomly distribute in the microstructure. Moreover, diopside crystalline phase has proper susceptibility for machining [23].

4. Conclusion

This study examined the sintering behavior and mechanical properties of glass–ceramics with two types of glass frits (G1: SiO_2–Al_2O_3–MgO–K_2O–F and G2: SiO_2–CaO–Na_2O). The sinterability of mica-based glass enhanced with gradual addition of G2 glass up to 30 wt.%. Further incorporation of G2 glass impeded densification due to precipitation of diopside crystalline phase.

Mechanical properties of sintered samples showed an incremental trend until 30 wt.% G2 glass portion. Excessive amount of G2 glass deteriorated some mechanical properties as a result of porosity that formed during crystallization of diopside. In addition, lower content of mica crystals decreased machinability.

The glass–ceramic with initial composition of 70 wt.% G1 and 30 wt.% G2 glass powder, demonstrated an ability of good machinability as well as high mechanical properties. Furthermore our results confirmed that above-mentioned composition reached to 98% relative density which represented desirable sinterability in pressureless sintering method. The microstructure of such specimen consisted of plate-like mica crystals and diopside needles.

References

[1] P.W. McMillan, Glass–Ceramics, second ed., Academic Press, London, 1979
[2] D.S. Baik, K.S. No, J.S. Chun, Y.J. Yoon, Mechanical properties of mica glass–ceramics, Journal of the American Ceramic Society 78 (5) (1995) 1217–1222.
[3] C.K. Chyung, G.H. Beall, D.G. Grossman, Microstructures & mechanical properties of mica glass–ceramics, in: M. Kunugi, M. Tashiro, N. saga (Eds.), Tenth International Congress on Glass. Part II, The Ceramic Society of Japan, Kyoto, Japan, 1974, pp. 1167–1194.
[4] C.K. Chyung, G.H. Beall, D.G. Grossman, Fluorphlogopite mica glass–ceramics, in: Proceeding of the International Glass Congress. No 14, The Ceramic Society of Japan, 1974, pp. 33–40.
[5] T. Uno, T. Kasuga, K. Nakajima, High strength mica-containing glass–ceramics, Journal of the American Ceramic Society 74 (1991) 3139–3141.
[6] T. Uno, T. Kasuga, S. Nakayama, Preparation of high-strength calcium mica-containing machinable glass–ceramics, Journal of the Ceramic Society of Japan 100 (1992) 703–707.
[7] H. Li, J. Ran, L. Gou, F. wang, Strengthening and toughening of mica-based machinable glass–ceramics, Rare Metal Materials Engineering 31 (2002) 514.
[8] H. Li, Q. You, L. Zhou, J. Ran, Study on machinable glass–ceramic containing fluorphlogopite for dental CAD/CAM system, Journal of Materials Science: Materials in Medicine 11 (2006) 1133–1137.
[9] O. Abe, K. Kourin, Strengthening of machinable glass–mica composites, Journal of the Ceramic Society of Japan 115 (2007) 216–221.
[10] M. Montazerian, P. Alizadeh, B. Eftekhari Yekta, Pressureless sintering and mechanical properties of mica glass–ceramic/Y-PSZ composites, Journal of the European Ceramic Society 28 (2008) 2687–2692.
[11] K. Cheng, J. Wan, K. Liang, Enhanced mechanical properties of oriented mica glass–ceramics, Materials Letters 39 (1999) 350–353.
[12] S. Habelitz, G. Carl, C. Rüssel, Processing, microstructure and mechanical properties of extruded mica glass–ceramics, Materials Science and Engineering A 307 (2001) 1–14.
[13] P. Alizadeh, B. Eftekhari Yekta, T. Javadi, Sintering behaviour and mechanical properties of the mica-diopside machinable glass–ceramics, Journal of the European Ceramic Society 28 (2008) 1569–1573.
[14] P. Alizadeh, V.K. Marghussian, Mechanical properties and bioactive characteristics of glass–ceramics, Journal of the American Ceramic Society Bulletin 81 (93) (2002) 21–26.
[15] B. Eftekhari Yekta, S. Hashemi Nia, P. Alizadeh, Influence of TiO_2, Cr_2O_3 and ZrO_2 on sintering and machinability of fluorophlogopite glass–ceramics, British Ceramic Transactions 103 (2004) 235–237.
[16] E.M. Rabinovich, Review: preparation of glass by sintering, Journal of Materials Science 20 (1985) 4259–4297.
[17] M. Sathiyakumar, F.D. Gnanam, Role of wollastonite additive on density, microstructure and mechanical properties of alumina, Ceramics International 29 (2002) 869–873.
[18] K. Cheng, J. Wan, K. Liang, Differential thermal analysis on the crystallization kinetics of K_2O–B_2O_3–MgO–Al_2O_3–SiO_2–TiO_2–F glass, Journal of the American Ceramic Society 82 (5) (1999) 1212–1216.
[19] R. Damani, R. Gstrein, R. Danzer, Critical notch-root radius effect in SENB-S fracture toughness testing, Journal of the European Ceramic Society 16 (1996) 695–702.
[20] C. Klein, Mineral Science, second ed., John Wiley and Sons, 2001.
[21] D.S. Baik, K.S. No, J.S. Chun, Effect of the aspect ratio of mica crystals and crystallinity on the microhardness and machinability of mica glass–ceramics, Journal of Materials Processing Technology 67 (1997) 50–54.
[22] D.G. Grossman, Machinable glass–ceramics based on tetrasilisic mica, Journal of the American Ceramic Society 55 (1972) 446–449.
[23] M. Taira, M. Yamaki, Phase constitution and microstructural characterisation of machinable glass–ceramic, British Ceramic Transactions 94 (3) (1995) 109–111.